# CrystEngComm

Accepted Manuscript






ROYAL SOCIETY OF CHEMISTRY

www.rsc.org/crystengcomm

# Anion Triggered and Solvent Assisted Structural Diversity and Reversible Single Crystal to Single Crystal (SCSC) transformation between 1D and 2D Coordination Polymers

Sarita Tripathi, Renganathan Srirambalaji, Samir Patra and Ganapathi Anantharaman[a]*

[a] Department of Chemistry, Indian Institute of Technology, Kanpur-208016, INDIA

**Abstract**

An anion induced structural variation from 1D to 2D was studied for four coordination polymers (CPs) synthesized from angular ditopic ligand 2,6-bis(imidazol-1-yl)pyridine ($pyim_2$) under different solvent conditions $\{[Zn(pyim_2)_2]\cdot(PF_6)_2\}_n$ (**1**) (1D), $\{[trans\text{-}Cd(pyim_2)_2(DMF)_2]\cdot(PF_6)_2\cdot(DMF)_2\}_n$ (**2**) (1D), $\{[trans\text{-}Cd(pyim_2)_2(H_2O)_2]\cdot(NO_3)_2\}_n$ (**3**) (2D) and $\{[trans\text{-}Cd(pyim_2)_2(H_2O)_2]\cdot(PF_6)\cdot(NO_3)\cdot(H_2O)_2\}_n$ **(4)** (1D). An anion triggered single crystal to single crystal (SCSC) transformation was observed from 1D to 2D by exchange of counter anion from $PF_6^-$ to $NO_3^-$ and vice versa. In addition the cause for SCSC transformation involving metal-ligand bond breaking/making phenomenon and enhancement/decrement of the network dimensionality is discussed. The anion/solvent exchange transformations were confirmed directly through single crystal X-ray diffraction, IR spectra, PXRD and elemental analysis. Furthermore thermal and solid state photoluminescence properties of **1**-**4** were analyzed.

## Introduction

Coordination polymers (CPs) showing dynamic nature are an area of profound interest since these CPs due to their structural flexibility, unlike rigid CPs, can undergo selective molecular recognition, guest/anion exchange and separation by tuning their cavity according to the guest molecules.[1-6] Recently the single-crystal to single-crystal (SCSC) transformation in dynamic CPs has received considerable attention as they exhibit structural changes associated with coordination and dimensionality. The SCSC transformations are induced by external stimuli such as temperature, solvent, anion and light.[7-11] In CPs SCSC transformation is challenging because it has to operate through the breaking and formation of coordinate and/or covalent bonds in the entire network without losing its crystallinity. However, very few transformations are known which involve the first coordination sphere of the metal centre, where the structural transformations are observed due to change in metal coordination environment and are mainly associated with the anion or solvent exchange.[12-15]

Recently anionic effects in the synthesis of CPs have been studied as they can be potentially employed as anion exchange materials.[16-25] The counter anions also act as a template in forming novel inorganic-organic hybrid architectures[16-17,26] and are responsible for binding together the chains or frameworks by weak non-covalent interactions such as hydrogen bonding and anion-$\pi$ interactions.[27-31] Although solvent/guest molecules or external stimuli assisted reversible SCSC transformations are known, so far very few examples of anion triggered reversible SCSC transformations are reported wherein the structural transformations are associated with the change in metal coordination environment and dimensionality (from lower to higher and vice versa), as it involves the breaking and formation of ligand to metal coordination/covalent bonds which is a difficult phenomenon in such extended networks.[32] It is

to be noted that SCSC transformations via anion exchange is somewhat hard to achieve as the charge and size of the anion plays a significant role in maintaining the integrity of the architecture and any change in them can collapse the entire framework.

Recently we and others are engaged in the synthesis of CPs showing structural diversity which are derived from angular ditopic ligands separated by the central five or six-membered heterocyclic rings.[33-37,41] Earlier, we have reported the synthesis of chiral and achiral 2D double helical CPs constructed from angular ditopic achiral ligand 2,6-bis(imidazol-1-yl)pyridine ($pyim_2$; Scheme 1) with group 12 metal ions where the variation in solvent conditions played a key role in formation of chiral CP through spontaneous resolution.[37] The change of anion from $NO_3^-$ to $PF_6^-$ can impart structural variability to the resulting CPs and to understand this effect we have incorporated $KPF_6$ in the reaction. Therefore, in order to understand the combined effects of the solvent and anions, particularly in the context of growth of CPs and dimensionality, we have been engaged in the synthesis of different CPs by varying the counter anions under different solvent conditions.

In this paper, we report the room temperature synthesis of four CPs $\{[Zn(pyim_2)_2]\cdot(PF_6)_2\}_n$ (**1**) (1D), $\{[trans\text{-}Cd(pyim_2)_2(DMF)_2]\cdot(PF_6)_2\cdot(DMF)_2\}_n$ (**2**) (1D), $\{[trans\text{-}Cd(pyim_2)_2(H_2O)_2]\cdot(NO_3)_2\}_n$ (**3**) (2D) and $\{[trans\text{-}Cd(pyim_2)_2(H_2O)_2]\cdot(PF_6)\cdot(NO_3)\cdot(H_2O)_2\}_n$ **(4)** (1D) from $pyim_2$. CP **2** shows dynamic behavior and in reversible SCSC manner is transformed to CP **3** via the exchange of coordinated solvent and counter anion, while CP **4** shows irreversible SCSC transformation to CP **3** via anion exchange, and these transformations resulted into change in the dimensionality from 1D to 2D and vice versa. The anion exchange was confirmed through Single crystal X-ray diffraction, PXRD patterns, elemental analysis and IR

spectroscopy. In addition, the photoluminescence behavior and thermal stability of these complexes were analyzed.

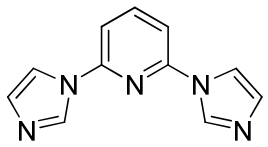

**Scheme 1.** 2,6-bis(imidazol-1-yl)pyridine ($pyim_2$)

**Experimental section**

**Materials and General procedures**

The ligand, $pyim_2$ was prepared according to the literature procedure.[38] $Zn(NO_3)_2 \cdot 6H_2O$ and $Cd(NO_3)_2 \cdot 4H_2O$ were obtained from SDFCL, India. All chemicals were used without further purification. Solvents were first dried and used after distillation. Elemental analyses were performed with an EAI Exeter analytical, INC CE-440 Elemental analyzer. IR spectra were recorded by using KBr pellets in the region 400-4000 $cm^{-1}$ on Bruker model vertex 70. NMR was recorded on JEOL ECX-500. Single crystal X-ray data for complexes **1-4** were collected at 293K (**1-3**) and 100 K (**4**) on a Bruker SMART APEX CCD diffractometer using graphite monochromated MoK$\alpha$ radiation ($\lambda$ = 0.71073 Å). Thermogravimetric analyses were done in $N_2$ atmosphere with a heating rate of 10 ˚C/min on Mettler Toledo Star System. Powder X-ray Diffraction (PXRD) data were collected on a PANalytical X'Pert Pro X-ray diffractometer with Cu K$\alpha$ radiation ($\lambda$ = 1.540598 Å) with a scan rate of 3˚/min at 293K. Solid state emission spectra were recorded using a ZSX primus series, Rigaku corporation spectrometer, at room temperature. DIAMOND (version 3) and Mercury (version 3.0) were used to view and draw the structures. Topological analysis of CP **3** was performed using the ADS program of the TOPOS 4.0 Professional structure-topological program package.[39]

**Synthesis of CPs 1-4**

**Synthesis of $\{[Zn(pyim_2)_2]\cdot(PF_6)_2\}_n$ (1).** To a solution of $Zn(NO_3)_2\cdot 6H_2O$ (0.029 g, 0.1 mmol) in distilled water (3 mL), a solution of $pyim_2$ (0.042 g, 0.2 mmol) in methanol (2 mL) was layered. Further, a solution of $KPF_6$ (0.037 g, 0.2 mmol) in distilled $H_2O$ (2 mL) was layered over the top of this solution. The solution was allowed to stand at RT to afford colorless crystals in three days. Yield: 0.058 g, 76% based on $Zn(NO_3)_2\cdot 6H_2O$. Elemental analysis (%) for $C_{22}H_{18}F_{12}N_{10}P_2Zn$ (777.77): Calcd. C, 33.97; H, 2.33; N, 18.01. Found: C, 33.94; H, 2.30; N, 18.03. IR (KBr, $cm^{-1}$): 3423 (br), 3166 (w), 1608 (s), 1588 (m), 1511 (s), 1461 (s), 1392 (w), 1340 (w), 1325 (m), 1291 (m), 1246 (s), 1182 (w), 1143 (br), 1116 (wm), 1084 (m), 1069 (s), 1010 (m), 968 (w), 948 (w), 835 (vs), 807 (s), 764 (m), 742 (s), 676 (br), 657 (m), 624 (w), 557 (s).

**Synthesis of $\{[Cd(pyim_2)_2(DMF)_2]\cdot(PF_6)_2\cdot(DMF)_2\}_n$ (2).** To a solution of $Cd(NO_3)_2\cdot 4H_2O$ (0.031 g, 0.1 mmol) in DMF (1 mL), a solution of $pyim_2$ (0.042 g, 0.2 mmol) in methanol (2 mL) was layered. Further, a solution of $KPF_6$ (0.037 g, 0.2 mmol) in $H_2O$ (2 mL) was layered over the top of this solution. The solution was allowed to stand at RT to afford colorless crystals in two days. Yield: 0.097 g, 44% based on $Cd(NO_3)_2\cdot 4H_2O$. Elemental analysis (%) for $C_{34}H_{46}CdF_{12}N_{14}O_4P_2$ (1117.19 g): Calcd. C, 36.55; H, 4.15; N, 17.55. Found: C, 36.52; H, 4.12; N, 17.51. IR (KBr, $cm^{-1}$): 3268 (w), 3156 (w), 3124 (m), 3089 (w), 1671 (br), 1604 (vs), 1588 (m), 1491 (vs), 1462 (vs), 1350 (vs), 1320 (s), 1287 (s), 1253 (m), 1241 (s), 1235 (vs), 1180 (w), 1135 (w), 1112 (w), 1103 (w), 1078 (m), 1065 (s), 1006 (m), 992 (w), 963 (w), 927 (m), 867 (w), 829 (m), 803 (s), 778 (br), 764 (m), 739 (w), 675 (br), 656 (s), 620 (w), 558 (br), 535 (br).

**Synthesis of $\{[trans\text{-}Cd(pyim_2)_2(H_2O)_2]\cdot(NO_3)_2\}_n$ (3).** To a solution of $Cd(NO_3)_2\cdot 4H_2O$ (0.154 g, 0.5 mmol) in $H_2O$ (3 mL), a solution of ethylenediamine (0.03 mL, 0.05 mmol) in $H_2O$ (2 mL) was added followed by a solution of $pyim_2$ (0.211 g, 1.0 mmol) in methanol (5 mL). The solution was allowed to stand at RT to afford colorless crystals in one week. Yield: 0.056 g, 36% based

on $Cd(NO_3)_2 \cdot 4H_2O$. Elemental analysis (%) for $C_{22}H_{22}CdN_{12}O_8$ (694.92): Calcd. C, 38.03; H, 3.19; N, 24.19. Found: C, 38.01; H, 3.14; N, 24.15. IR (KBr, $cm^{-1}$): 3411(s), 3157(m), 3124 (m), 1674 (w), 1605 (vs), 1589 (s), 1491 (vs), 1463 (vs), 1385 (s), 1345 (s), 1289 (s), 1253 (s), 1242 (s), 1180 (s), 1137 (w), 1111 (m), 1079 (m), 1068 (s), 1005 (s), 992 (w), 963 (m), 927 (m), 868 (m), 803 (s), 762 (m), 676 (w), 656 (s), 619 (w), 535 (w).

**Synthesis of $\{[trans\text{-}Cd(pyim_2)_2(H_2O)_2]\cdot(PF_6)\cdot(NO_3)\cdot(H_2O)_2\}_n$ (4).** To a solution of $Cd(NO_3)_2 \cdot 4H_2O$ (0.031 g, 0.1 mmol) in DMF (1 mL), a solution of $pyim_2$ (0.042 g, 0.2 mmol) in methanol (2 mL) was layered. Further, a solution of $KPF_6$ (0.037 g, 0.2 mmol) in $H_2O$ (2 mL) was layered over the top of this solution followed by $H_2O$ (8 mL) was layered over all the solution. The solution was allowed to stand at RT to afford colorless crystals in six days. Yield: 0.056 g, 63% based on $Cd(NO_3)_2 \cdot 4H_2O$. Elemental analysis (%) for $C_{22}H_{26}CdF_6N_{11}O_7P$ (813.88): Calcd. C, 32.47; H, 3.22; N, 18.93. Found: C, 32.39; H, 3.20; N, 18.88. IR (KBr, $cm^{-1}$): 3601 (m), 3400 (m), 3157 (m), 1649 (m), 1607 (vs), 1590 (s), 1527 (m), 1496 (vs), 1463 (vs), 1384 (vs), 1306 (s), 1278 (s), 1261 (s), 1239 (s), 1174 (m), 1144 (br), 1131 (br), 1106 (m), 1071 (s), 1060 (s), 1012 (s), 965 (w), 932 (m), 843 (vs), 802 (vs), 765 (s), 745 (m), 675 (w), 648 (s), 622 (w), 557 (s), 436 (br).

**SCSC transformation of CP 2 to CP 3.** Single crystals of CP **2** were immersed in an aqueous solution of $NH_4NO_3$ (0.1 mmol, 8 mg) for one week to give CP **3**.

**SCSC transformation of CP 3 to CP 2.** Single crystals of CP **3** were immersed in MeOH/DMF/$H_2O$ (1/0.5/1) solution of $KPF_6$ (0.1 mmol, 18 mg) for two weeks to give CP **2**.

**SCSC transformation of CP 4 to CP 3**. Single crystals of CP **4** were immersed in an aqueous solution of $NH_4NO_3$ (0.1 mmol, 8 mg) for one week to give CP **3**.

**X-ray Crystallography.** Single crystal X-ray data for **1-4** were collected at 293K (**1-3**) and 100 K (**4**) on a Bruker SMART APEX CCD diffractometer using graphite monochromated $MoK_\alpha$ radiation ($\lambda$ = 0.71073 Å). All the structures were solved using SHELXS-97 and refined by full-matrix least squares on $F^2$ using SHELXL-97.[40-41] All hydrogen atoms were included in idealized positions using a riding model. Non-hydrogen atoms were refined with anisotropic displacement parameters. The hydrogen atoms of water molecules in CP **4** were located from difference Fourier maps and the O–H bond distances constrained to ~0.80–0.90 Å with the DFIX command.

**Results and discussion**

CPs **1-4** were synthesized via layering method under different solvent conditions and by using a mixture of solvent systems. In case of CP **1** and **3** only the polar protic solvents ($H_2O$/MeOH) were used, while CPs **2** and **4** were prepared by using both polar protic as well as polar aprotic solvents ($H_2O$/MeOH/DMF). The difference in the solubility of the hydrophilic or hydrophobic anions was considered during the reaction while varying the quantity of solvents. All the CPs (**1-4**) were insoluble in common organic solvents and the structures were confirmed through single crystal X-ray diffraction. In addition to IR and elemental analysis PXRD was carried out to check the bulk purity of the samples.

**$\{[Zn(pyim_2)_2]\cdot(PF_6)_2\}_n$ (1).** Single crystal X-ray diffraction study reveals that **1** crystallizes in triclinic space group *P*-1 (Table 1). **1** forms a 1D chain and consists of a $ZnN_4$ tetrahedral unit, where zinc is coordinated by four different imidazole nitrogen atoms of $pyim_2$ (Figure 1a). **1** consists of two $PF_6^-$ counter anions confirmed through IR spectrum showing stretching peaks at 835 $cm^{-1}$ and 557 $cm^{-1}$ corresponding to $PF_6^-$ ions. As compared to the previously reported Zn(II) octahedral CP $\{[trans\text{-}Zn(pyim_2)_2(H_2O)_2]\cdot(NO_3)_2\}_n$ with $pyim_2$ being *trans* to each other and

nitrate as counter anion,[37] by changing the solvent conditions to more polar protic one and counter anion to $PF_6^-$ the geometry around Zn(II) changes to tetrahedral in **1**. The average Zn-N bond length is 2.013(7) Å and is consistent with those of reported values in literature.[42] In **1**, two $pyim_2$ units further coordinate to another Zn (II) unit resulting into a 1D chain CP (Figure 1b). The adjacent loops $[Zn_2(pyim_2)_2]$ are oriented perpendicular to each other with a variable Zn···Zn distance observed as 8.75(6) Å and 8.96(9) Å. $PF_6^-$ ions are occupied inside the loops and along the grooves in an alternating fashion resulting in 1D chain. In **1**, the C-N bond rotation due to deviation of one of the imidazole ring from the plane of the pyridine ring results into an interplanar angle of 37.31(6)°, while $pyim_2$ exhibits *cis-cis* conformation with an N···N···N angle of 126.48(6)° (N5···N3···N1) and 124.35(5)° (N9···N8···N6). The additional stability to the 1D chain in **1** is provided through H-bonding interactions existing between non coordinating $PF_6^-$ ions and C-H of imidazole from two different 1D chains (Figure 1c, Table 3) leading to a 2D supramolecular network (Figure 1d).

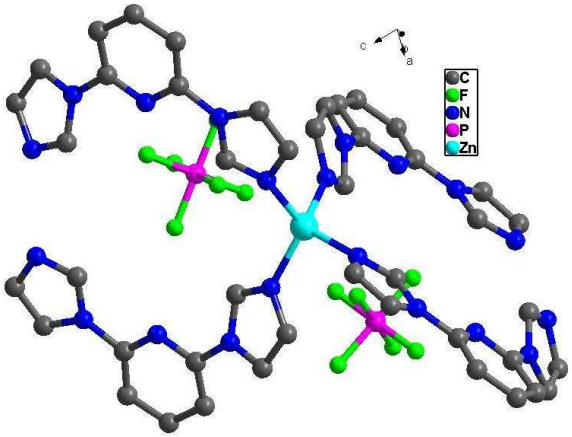


(a)

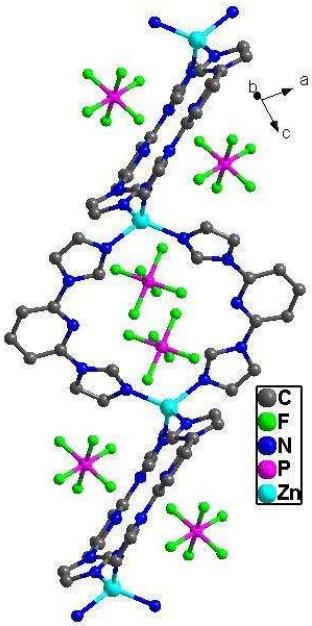


(b)

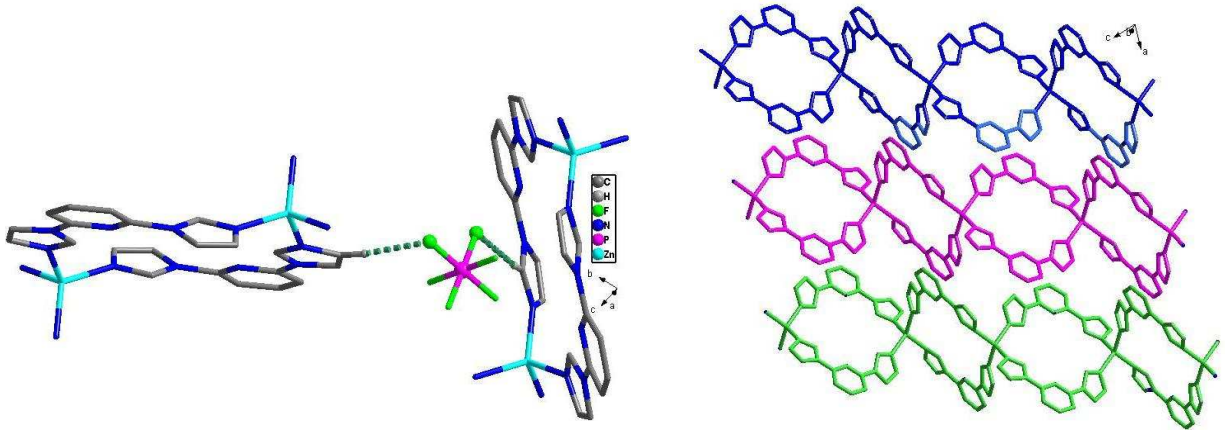


(c) (d)

**Figure 1.** (a) The coordination environment around Zn(II) ion with counter anions in **1** (H-atoms omitted for clarity). (b) 1D chain of **1** showing position of $PF_6^-$. (c) H-bonding interactions between two independent chains in **1**. (d) 2D supramolecular architecture of **1**.

**$\{[Cd(pyim_2)_2(DMF)_2]\cdot(PF_6)_2\cdot(DMF)_2\}_n$ (2).** Single crystal X-ray diffraction study reveals that **2** crystallizes in monoclinic space group $P2_1/n$ (Table 1). In **2**, Cd(II) centre lies in an octahedral geometry and is coordinated to four different imidazole nitrogen atoms of $pyim_2$ present in the plane while the axial positions are occupied by two DMF molecules (Figure 2a). **2** consist of two $PF_6^-$ counter anions, confirmed through IR spectrum exhibiting stretching peaks at 829 $cm^{-1}$ and 558 $cm^{-1}$, along with two DMF guest molecules present as solvent of crystallization. The average Cd-N and Cd-O bond distances are 2.308(7) Å and 2.375(1) Å respectively and are consistent with the reported values in literature.[43-44] Two $pyim_2$ units further coordinate to another Cd(II) unit leading to a 1D chain CP (Figure 2b). In the 1D chain, the Cd···Cd distance is 11.08(3) Å and unlike **1**, in **2** the $PF_6^-$ ions are present only inside the loops. Furthermore, these $PF_6^-$ ions are held within the loop through anion-$\pi$ interactions between F9 and F12 and the pyridine rings (Figure 2c). Like **1**, the C-N bond rotation in **2**, results into deviation of one of the imidazole ring from the plane of the pyridine ring with an interplanar angle of 21.00(2)°. In **2**, the *cis-trans*

conformation was observed for $pyim_2$ and N···N···N angle was found to be 141.67 (1)° and 141.50(1)° for N5···N3···N1 and N10···N8···N6 respectively. The 1D chains are further stabilized through $\pi$-$\pi$ stacking between pyridine and imidazole rings as well as two imidazole rings (Figure 2d). The distance between pyridine and imidazole rings ranges from 3.326(1)-3.333(2) Å, centroid to centroid distance is 3.946(2) Å and angle between the planes is 0.574(1)°. The distance between two stacked imidazole rings is in the range of 3.046(1)-3.295(8) Å, centroid to centroid distance is 3.920(8) Å and angle between the planes is 17.194(2)°. These $\pi$-$\pi$ interactions lead to a 2D supramolecular arrangement of this 1D CP chain.

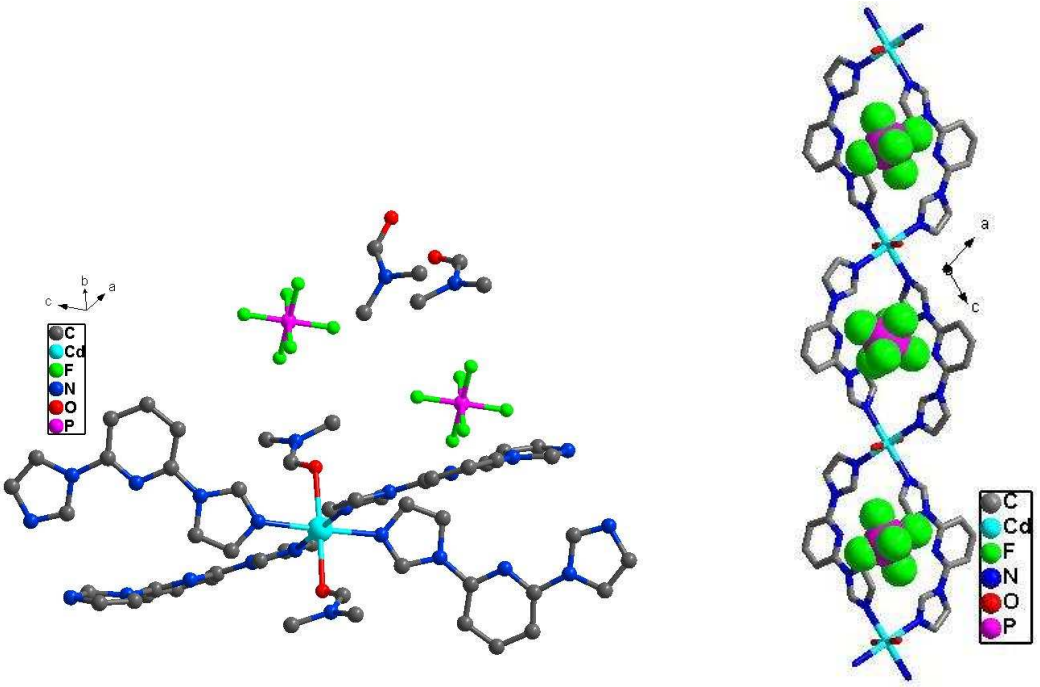


(a) (b)

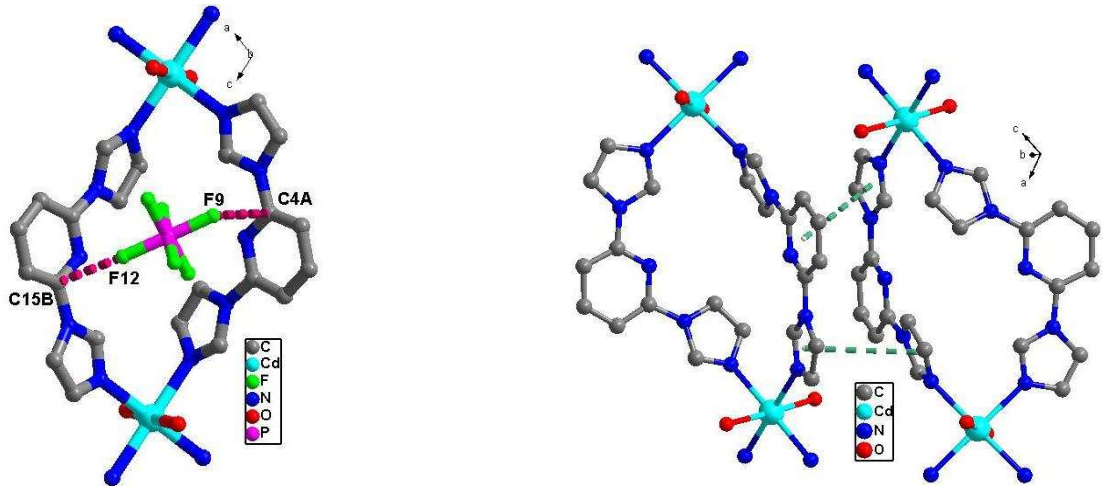


(c) (d)

**Figure 2.** (a) The coordination environment around Cd(II) ion with counter anions in **2** (H-atoms omitted for clarity). (b) 1D chain of **2** showing position of $PF_6^-$. (c) Anion-$\pi$ interactions within the loop in **2** where C4A···F9 = 3.139(7) Å; F···centroid distance = 3.451(3) Å and C15B···F12 2.977(4) Å; F···centroid distance = 3.006(5) Å. [C4A is at x, y, 1 + z and C15B is at 1/2 + x, 1/2 - y, 1/2 + z]. (d) $\pi$-$\pi$ interactions between two independent chains in **2**.

**{[*trans*-Cd(pyim$_2$)$_2$(H$_2$O)$_2$]·(NO$_3$)$_2$}$_n$ (3).** **3** crystallizes in monoclinic space group $P2_1/c$ and is isostructural to previously reported {[*trans*-Zn(pyim$_2$)$_2$(H$_2$O)$_2$]·(NO$_3$)$_2$}$_n$.[37] It consists of a similar geometrical arrangements consisting of Cd(II) in octahedral geometry (present at an inversion centre), with two nitrate counter anions (Figure 3a-b) confirmed by IR spectrum showing a strong peak at 1385 cm$^{-1}$ corresponding to $NO_3^-$ ions. The average Cd-N and Cd-O bond distances are 2.333(1) Å and 2.317(7) Å respectively and are consistent with the reported values in literature.[43-44] In the 2D double helix the Cd···Cd distance is 9.36(9) Å and 9.50(8) Å. The C-N bond rotation results into an interplanar angle of 25.65(1)° which influences further twist of these rings and thereby initiating the helicity. In **3**, the *cis-cis* conformation was observed for pyim$_2$ and N···N···N angle was found to be 126.69(8)°. Through topological

analysis, **3** can be represented as $4^4.6^2$ sql tetragonal plane net with Cd centre as 4-connected uninodal net (Figure 3c). The additional stability to the double helix is provided by one of the oxygen atoms O3, from nitrate ion showing O-H···O as well as C-H···O hydrogen bonding interactions with the axially coordinated water molecule and C-H of imidazole respectively (Figure 3d, Table 3). It connects two independent 2D double helical chains of **3** and leads to the formation of a 3D supramolecular network.

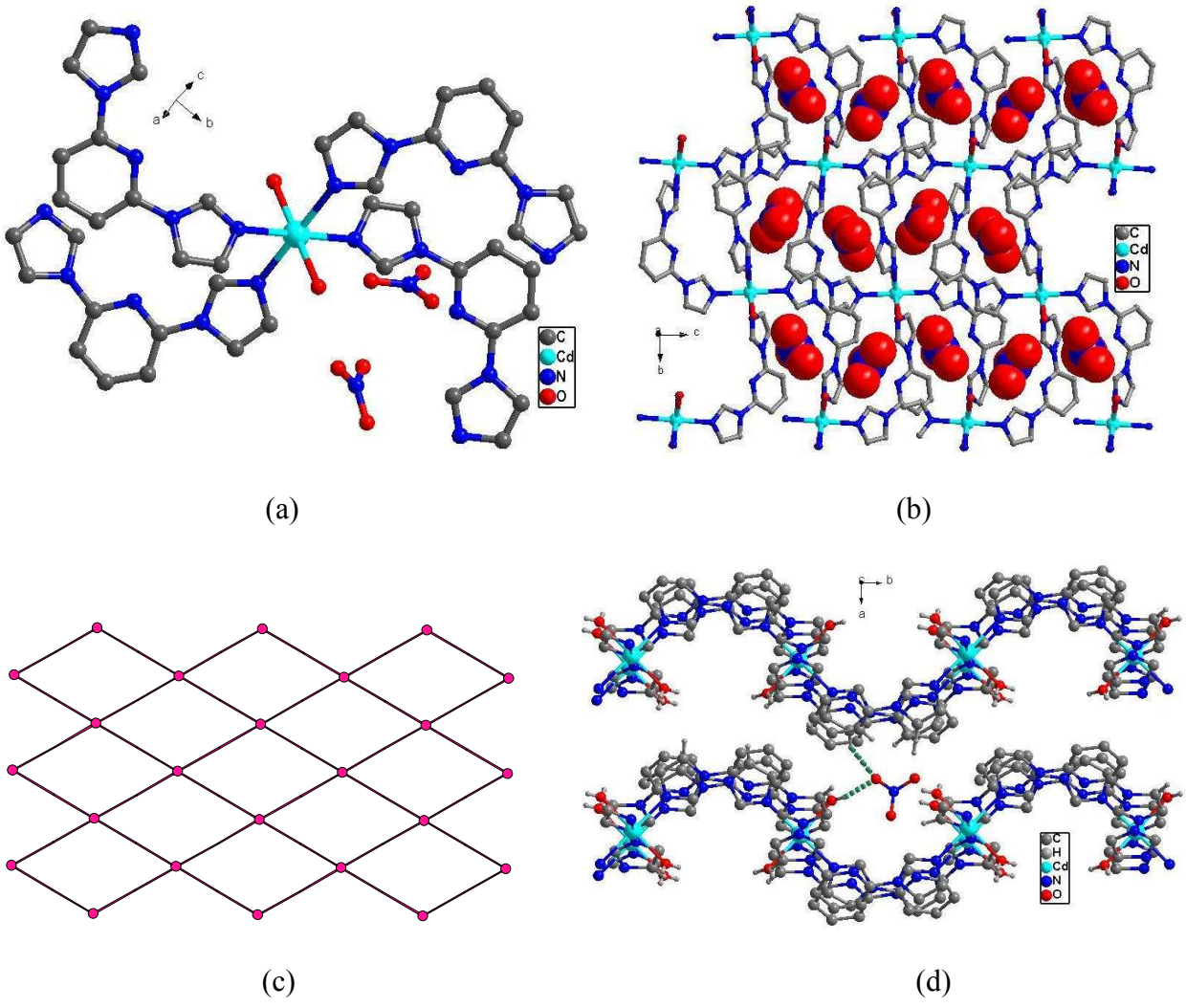


(a) (b)

(c) (d)

**Figure 3.** (a) The coordination environment around Cd(II) ion with counter anions in **3** (H-atoms omitted for clarity). (b) 2D double helix of **3** showing position of $NO_3^-$. (c) Topological

representation of 4-connected nodes in **3**. (d) H-bonding interactions between two independent double helix through $NO_3^-$ in **3**.

**{[Cd(pyim$_2$)$_2$(H$_2$O)$_2$]·(PF$_6$)·(NO$_3$)·(H$_2$O)$_2$}$_n$ (4).** Single crystal X-ray diffraction study reveals that **4** crystallizes in monoclinic space group $P2_1/n$ (Table 1). It consists of Cd(II) octahedral geometry (present at an inversion centre), where cadmium is coordinated to four different imidazole nitrogen atoms of $pyim_2$ present in the plane while the axial positions are occupied by two water molecules (Figure 4a). **4** consist of coexistent counter anions $NO_3^-$ and $PF_6^-$ along with two $H_2O$ molecules as solvent of crystallization. Both P1 of $PF_6^-$ and N6-O4 of the $NO_3^-$ are on a twofold axis. The coexistence of both counter anions was confirmed by IR spectrum showing strong peak at 1384 $cm^{-1}$ corresponding to $NO_3^-$ ions and stretching peaks at 843 $cm^{-1}$ and 557 $cm^{-1}$ corresponding to $PF_6^-$ ions. The average Cd-N and Cd-O bond distances are 2.330(3) Å and 2.373(5) Å respectively and are consistent with the reported values in literature.[43-44] In **4,** two of the individual $pyim_2$ units coordinate to another Cd(II) unit resulting into a 1D chain CP (Figure 4b) with a Cd···Cd distance as 11.22(1) Å. CP **4** comprises of both $NO_3^-$ and $PF_6^-$ ions where the $NO_3^-$ are present alongside the grooves while the $PF_6^-$ ions are present in the loops of the 1D chain. Furthermore, the $PF_6^-$ ions are held within the loops by anion-$\pi$ interactions with the pyridine ring through F3 and F4 (Figure 4c). The C-N bond rotation results into an interplanar angle of 23.31(9)° and N···N···N angle for $pyim_2$ was found to be 140.50(3)° with a *cis-trans* conformation. The additional stability to the 1D chain in **4** is provided through H-bonding interactions existing between axially coordinated water molecule, nitrate ion and lattice water molecule (Figure 4d, Table 3). The H-bonding operates in an interesting way where coordinated water molecule shows O-H···O interactions with lattice water molecule which in turn is connected to nitrate ion through O-H···O interactions. In this way the lattice water and nitrate

ion acts as a bridge between two independent 1D chains affording a 2D supramolecular architecture.

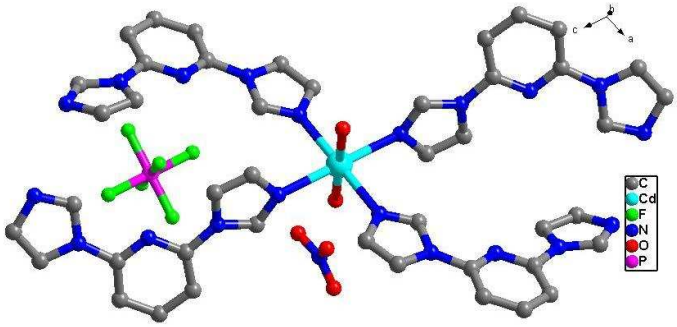


(a)

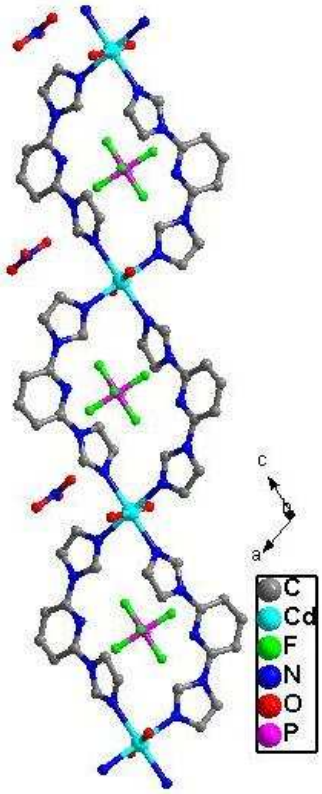


(b)

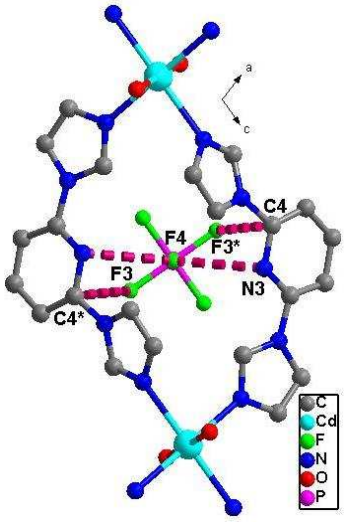


(c)

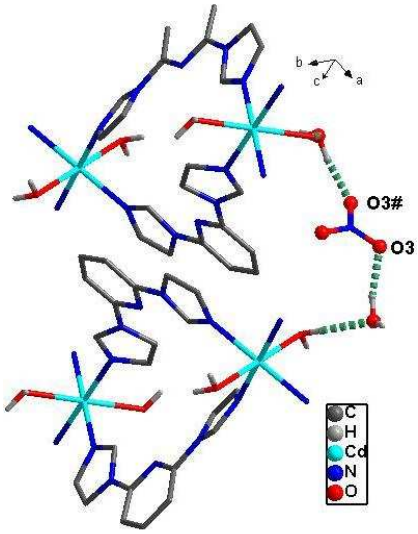


(d)

**Figure 4.** (a) The coordination environment around Cd(II) ion with counter anions in **4** (H-atoms omitted for clarity). (b) 1D chain of **4** showing position of $PF_6^-$ and $NO_3^-$. (c) Anion-$\pi$ interactions within the loop in **4** where C4···F3 = 3.094(9) Å; F···centroid of pyridine ring = 3.243(7) Å and N3···F4 3.016(2) Å; F···centroid distance = 3.854(2) Å. [C4* and F3* are at equivalent position: 3/2 - x, y, 1/2 - z]. (d) H-bonding interactions between two independent chains via $H_2O$ and $NO_3^-$ in **4**. O3# is at 3/2 - x, y, 3/2 – z.

**Anion triggered structural variation**

As it is evident by the structural variations in CPs **1-4**, the $PF_6^-$ counter anions in **1-2** form a 1D chain, while $NO_3^-$ counter anion forms a 2D double helical architecture in CP **3**. The variation in architecture can be due to difference in the size of these anions since the molecular volume of $PF_6^-$ (54 $Å^3$) is quite larger than that of $NO_3^-$ (34 $Å^3$)[45] and hence lead to 1D chain due to their position within the loops. The $NO_3^-$ ions on the other hand due to the smaller volume are occupied between the helices and allow for a 2D double helix. However, CP **4** consisting of both $NO_3^-$ and $PF_6^-$ counter anions leads to a 1D CP and can be considered as an intermediate between CPs **2** and **3**, which can be understood based on the supramolecular interactions shown by the counter anions. The analysis of the structure of CP **4** shows that the $PF_6^-$ anions are held within the loops by the anion-$\pi$ interactions and lead to a 1D chain, similar to CP **2**, while the $NO_3^-$ anions are present along the grooves and facilitate in stabilizing the 1D chains through H-bonding, similar to CP **3**. It further confirms that the anions tune the dimensionality leading to an anion controlled architectures in these CPs.

**Anion/solvent triggered SCSC transformation**

The anions occupied in the cavities of CPs are held together by weak interactions such as H-bonding and anion-$\pi$ interactions. These CPs can undergo anion exchange[27-31] and lead to the

formation of potential anion exchange materials.[18-25] Owing to this interest we have subjected CPs (**2-4**) for anion exchange as the anions were held inside the network though weak supramolecular interactions. The CPs were found to retain their crystalline nature when dipped in $H_2O$ or MeOH/DMF/$H_2O$ mixture and no exchange was observed in between the mentioned time period which was confirmed through single crystal X-ray diffraction. To our surprise reversible exchange of anions and coordinated solvent molecules at the metal centre occurred between CPs **2** and **3** in SCSC manner. In contrast, an irreversible SCSC anion exchange was observed from **4** to **3** (Figure 5). The SCSC transformations were authenticated by single crystal X-ray diffraction methods and in bulk they were further confirmed through IR, PXRD and elemental analysis.

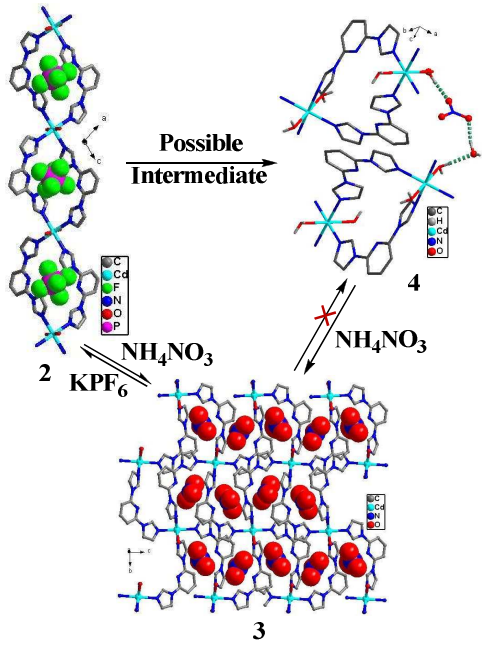


**Figure 5.** A schematic diagram illustrating the anion triggered SCSC transformations

The SCSC transformation of CP **2** to **3** resulted due to the exchange of $PF_6^-$ counter anions with $NO_3^-$ accompanied by replacing coordinated DMF with $H_2O$ molecules at the Cd(II) centre. The reversible SCSC transformation was also reported from **3** to **2** on account of change in counter anion from $NO_3^-$ to $PF_6^-$ accompanied by change at the metal coordination centre from

$H_2O$ to DMF. In CP **4** the irreversible transformation occurred by the exchange of counter anion $PF_6^-$ with $NO_3^-$. IR spectra after the transformation of **2** and **4** to **3** shows absence of $PF_6^-$ peaks and the appearance of absorption peak for $NO_3^-$ (Figures 6 and 8; spectrum in green color). While in **3** the SCSC transformation to **2** is confirmed through the presence of absorption peaks for $PF_6^-$ ions (Figures 7; spectrum in green color). The PXRD of transformed SCSC CP products matches well with that of the as synthesized one (Figures 9-11).

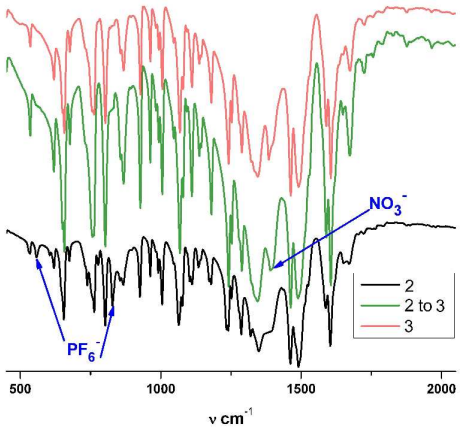


**Figure 6.** IR spectra of **2, 3 (**after SCSC transformation) and **3** (as synthesized)

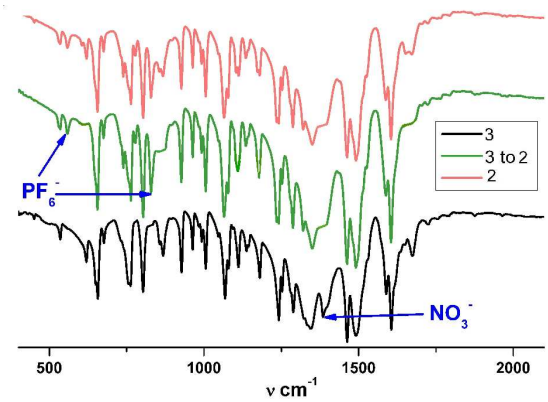


**Figure 7.** IR spectra of **3, 2 (**after SCSC transformation) and **2** (as synthesized)

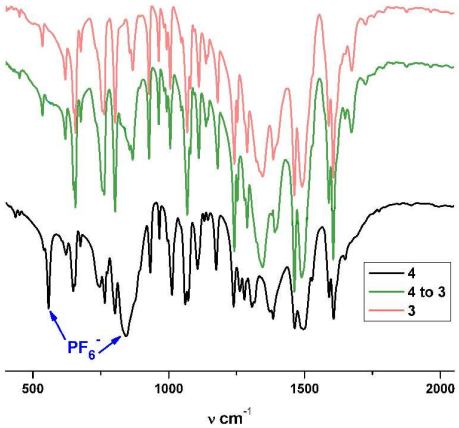


**Figure 8.** IR spectra of **4, 3 (**after SCSC transformation) and **3** (as synthesized)

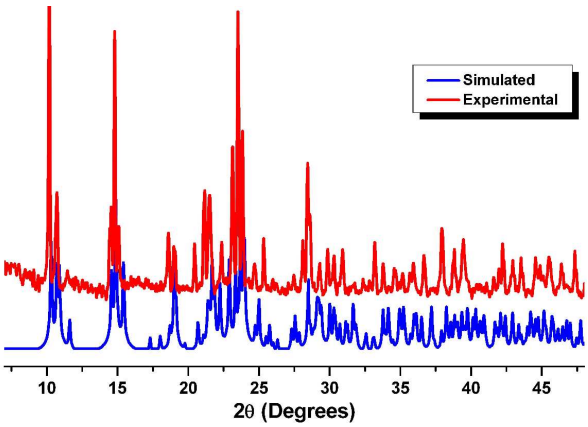


**Figure 9.** PXRD of **2** SCSC transformed to **3**

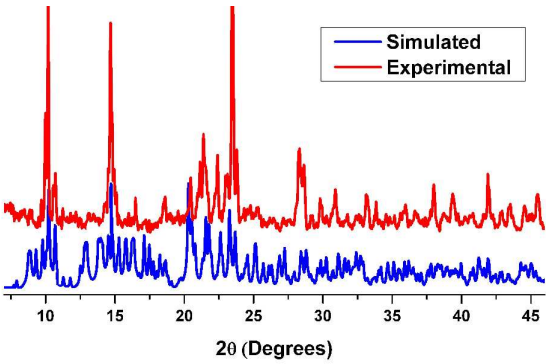


**Figure 10.** PXRD of **3** SCSC transformed to **2**

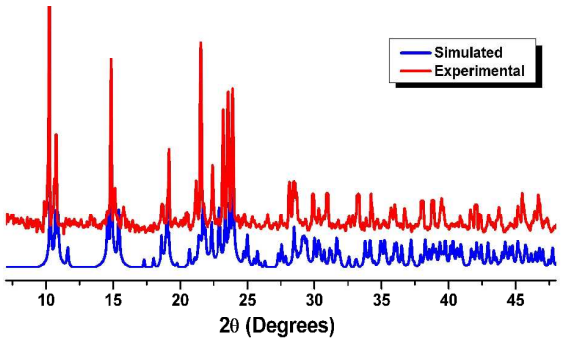


**Figure 11.**PXRD of **4** SCSC transformed to **3**

The reversible conversion from **2** to **3** in SCSC manner shows a dynamic anion exchange property of these CPs and are accompanied by the increase (from **2** to **3**) or decrease (from **3** to **2**) in the dimensionality from 1D to 2D and vice versa. Further, an irreversible dimensionality change occurs in transformation of **4** to **3**. The reversible transformations between **2** and **3** indicate the lability of weakly bound anions which upon the judicious choice of the solvent can be converted reversibly. The replacement of bulkier $PF_6^-$ by the smaller $NO_3^-$ from **2** to **3** is reflected in the resultant change in the crystallographic and structural parameters as it reduces the unit cell volume to almost one-third from 4536 $Å^3$ (**2**) to 1332 $Å^3$ (**3**). Moreover, the difference in the volume of the counter anion $PF_6^-$ imparts significant decrease in the Cd···Cd distance from ~11 Å in **2** to ~9 Å in **3**. This implies that the $PF_6^-$ ion occupied between the $Cd_2(pyim_2)_2$ loop with more space not only increases the distance between two Cd(II) centre, but also controls the dimensionality in **2**. The change in the dimensionality is assisted by the rotation of C–N bond to *cis-cis* orientation of imidazole rings in $pyim_2$ which subsequently distorts the coordination network and forces each units of $pyim_2$ to slide towards the Cd(II) centers of the neighboring layer to reduce the empty space and connect the two nearest neighbors in the same crystal to compensate for the reduction in volume. Usually, such changes occur in flexible CPs when an

increase of the network dimensionality occurs in order to reach the local energy minimum and results into the distortion of the whole network and local coordination geometry.

Furthermore if we inspect the structure of **4** then it is observed that the $PF_6^-$ ion has retained its position between the $Cd_2(pyim_2)_2$ loop similar to that of **2** (Figure 4c), with the difference that the $PF_6^-$ ions linking the inter-chain 1D CP are replaced by $NO_3^-$ ions. The former observation suggests that the transformation of **2** to **3** is probably going via **4** as an intermediate. Of the entire comparison one may puzzle the role of $NO_3^-$ and the $pyim_2$ ligand in these structural transformations. To understand the wider applicability of this SCSC transformation anion exchange in **1**-**4** with other anions such as $Cl^-$, $SO_4^{2-}$, $SO_3^{2-}$, $CO_3^{2-}$ and $BF_4^-$ is carried out. However these attempts were unsuccessful proving the selectivity of anions in these CPs.

**Thermogravimetric and Powder X-ray diffraction analyses**

The thermal stability of **1**-**4**, was studied using the thermogravimetric analysis (TGA) (Figure 12). The TGA profile of **1** indicated that it was thermally stable up to 320 $^{\circ}$C and then shows a sudden weight loss leaving residual weight of 47%. In case of **2,** the CP is thermally stable up to 124 $^{\circ}$C followed by a weight loss of approx. 5% corresponding to one DMF molecule (calculated, 6.5 wt %). Subsequently, a sequential weight loss starting at 290 $^{\circ}$C is observed (residue 35%). The TGA profile indicated that **3** is thermally stable up to 100 $^{\circ}$C after which the framework showed 4.8% weight loss corresponding to two coordinated water molecules (calculated, 5.18 wt %) and after 330 $^{\circ}$C a continuous weight loss is observed (residue 17%). Unlike **3**, the profile of **4** indicated that a continuous weight loss upto 6.6 % was observed and this can be attributed to the loss of three water molecules (calculated 6.6 wt %). **4** further shows a gradual weight loss after 224 $^{\circ}$C (residue 40%). To confirm the sample purity powder X-ray diffraction was performed for compounds **1**–**4** and it was observed that the simulated spectra

correlates with the experimental spectra which confirms the phase purity of these compounds at room temperature (Figure S1).

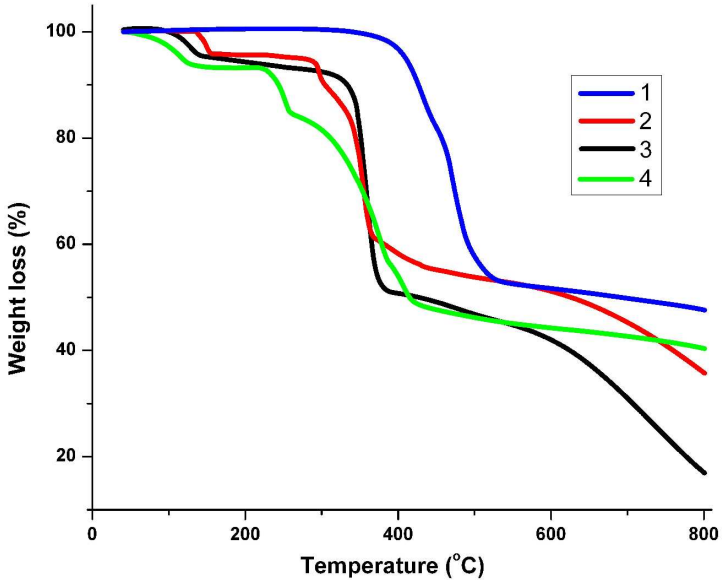


**Figure 12.** TGA curves of compounds **1-4**

**Photoluminescence**

CPs consisting of transition metals with $d^{10}$ electronic configuration such as Zn(II) and Cd(II) with suitable organic linkers are found to exhibit excellent photoluminescent properties.[46-47] Therefore the complexes synthesized by using these metal ions can be employed as new luminescent materials. Consequently, the photoluminescent properties of complexes **1-4** were investigated at room temperature (Figure 13). In the solid state, the free $pyim_2$ shows intense luminescence with emission maxima at 345 nm ($\lambda_{ex}$ 300 nm) due to the $\pi^*$-$\pi$ transition. Compounds **1-4** are red shifted from the ligand and exhibit emission at 393 nm ($\lambda_{ex}$ 295 nm), 434 nm ($\lambda_{ex}$ 280 nm), 439 nm ($\lambda_{ex}$ 280 nm) and 394 nm ($\lambda_{ex}$ 292 nm) respectively. The cause of red shift for compounds **1-4** can be attributed to ligand to metal charge transfer (LMCT) transition. The increased emission in complex **1** may be caused firstly due to the presence of $PF_6^-$ and secondly due to absence of any solvent molecules which rules out quenching by any high energy

bond vibration thereby increasing the intensity. The decrease in luminescence intensity of **2** and **3** can be attributed due to the presence of coordinated as well as free DMF (**2**) and coordinated $H_2O$ (**3**) which shows quenching due to high energy O-H and C-H vibrations respectively.[48-49] The increased emission in **4** in spite of having coordinated $H_2O$ molecules can be due to the presence of $PF_6^-$ since fluorine contributes in an increased intensity.

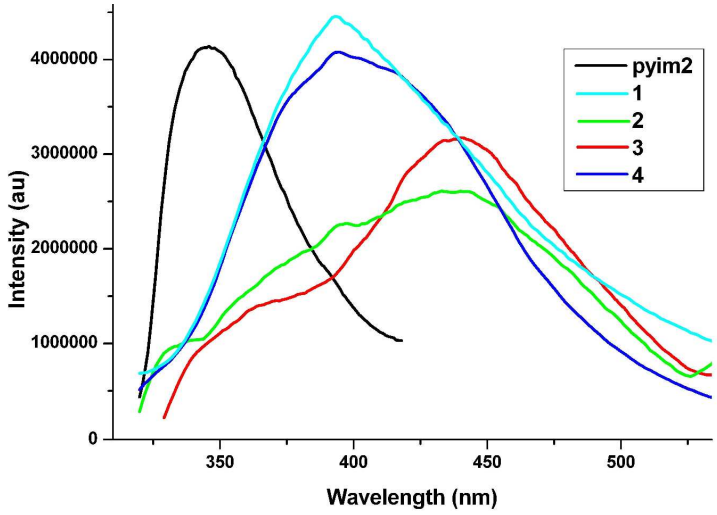


**Figure 13.** Solid state photoluminescence spectra of compounds **1-4**

## Conclusion

In conclusion, we have synthesized four new CPs $\{[Zn(pyim_2)_2]\cdot(PF_6)_2\}_n$ (**1**), $\{[trans\text{-}Cd(pyim_2)_2(DMF)_2]\cdot(PF_6)_2\cdot(DMF)_2\}_n$ (**2**), $\{[trans\text{-}Cd(pyim_2)_2(H_2O)_2]\cdot(NO_3)_2\}_n$ (**3**) and $\{[trans\text{-}Cd(pyim_2)_2(H_2O)_2]\cdot(PF_6)\cdot(NO_3)\cdot(H_2O)_2\}_n$ (**4**) from angular ditopic ligand $pyim_2$. The size of the anion plays a crucial role in modulating the structure and dimensionality of the CP as 1D ($PF_6^-$) or 2D ($NO_3^-$) and leads to the formation of CPs **1-2**, **4** as 1D chain while CP **3** as a 2D double helical chain. CPs **2** and **3** showed dynamic behavior by undergoing reversible anion exchange through SCSC transformation, while CP **4** was transformed to **3** via anion exchange in irreversible SCSC manner. The thermal and solid state photoluminescence property of CPs **1-4**

was also investigated. This study once again illustrates the importance of anion and solvent variations in the field of crystal engineering and enhancement/decrement of dimensionalities in the self assembled CPs using angular semi-rigid ligands. These CPs can be employed as anion exchange materials and the study is under progress.

**Associated Content**

**Electronic Supplementary Information (ESI)**

Powder X-ray diffraction patterns. X-ray crystallographic data in CIF format have been deposited with the Cambridge Structural Database. CCDC: 1041303-1041306 contains the supplementary crystallographic data for this paper.

**Author Information**

**Corresponding author**

***E-mail: garaman@iitk.ac.in**

**Acknowledgment**

The authors thank Council of Scientific and Industrial Research (CSIR), Department of Science and technology (DST), Government of India for financial support and Indian Institute of Technology (IIT), Kanpur for infrastructural facilities. Also we thank "Thematic Unit of Excellence on Soft Nanofabrication with Application in Energy, Environment and Bioplatform at IIT Kanpur" for PXRD facility. ST and RS thank CSIR and IITK respectively for their research fellowships.

**Table 1.** Crystallographic data and structural refinement summary of **1-4**

| | **1** | **2** | **3** | **4** |
|---|---|---|---|---|
| Empirical Formula | $C_{22}H_{18}N_{10}ZnF_{12}P_2$ | $C_{34}H_{46}N_{14}O_4CdF_{12}P_2$ | $C_{22}H_{22}N_{12}O_8Cd$ | $C_{22}H_{26}N_{11}O_7CdF_6P$ |
| Fw | 777.77 | 1117.19 | 694.92 | 813.91 |
| Crystal dimensions ($mm^3$) | 0.20×0.18×0.15 | 0.10×0.08×0.07 | 0.20×0.18×0.14 | 0.22×0.19×0.15 |
| Crystal system | Triclinic | Monoclinic | Monoclinic | Monoclinic |
| Space group | *P*-1 | *P* $2_1/n$ | *P* $2_1/c$ | *P* $2_1/n$ |
| *a*, Å | 9.979(5) | 11.5527(12) | 8.6147(6) | 11.915(3) |
| *b*, Å | 10.302(5) | 26.816(3) | 16.5484(12) | 8.1768(18) |
| *c*, Å | 15.743(5) | 15.4979(16) | 9.3691(7) | 15.913(4) |
| *α*, (°) | 80.924(5) | 90 | 90 | 90 |
| *β*, (°) | 73.374(5) | 109.134(2) | 93.617(1) | 106.617(4) |
| *γ*, (°) | 65.235(5) | 90 | 90 | 90 |
| *V*, $Å^3$ | 1406.8(11) | 4536.0(8) | 1332.99(17) | 1291.3(6) |
| *Z* | 2 | 4 | 2 | 2 |
| $\rho_{calcd}$, $mg/m^3$ | 1.836 | 1.636 | 1.731 | 1.820 |
| $\mu$, $mm^{-1}$ | 1.103 | 0.656 | 0.892 | 0.890 |
| *F*(000) | 776 | 2264 | 700 | 816 |
| *T* (K) | 293(2) | 293(2) | 293(2) | 100(2) |
| $\theta_{min/max}$ range (°) | 2.18-26.00 | 1.52-26 | 2.37-26 | 1.90-26 |
| Range of *h,k,l* | −12/11, −12/12, −16/19 | −14/13, −33/25, −19/18 | −10/8, −20/19, −11/11 | −14/14, −10/7, −17/19 |
| Reflections collected/unique | 7947/5378 | 25318 / 8885 | 7388/2604 | 7776/2879 |
| Data/ restraints /parameter | 5378/0/ 424 | 8885 / 0 / 612 | 2604 / 0 / 201 | 2879/3/ 235 |
| GOF on $F^2$ | 1.168 | 1.100 | 1.188 | 1.167 |
| $R_{int}$ | 0.0167 | 0.0620 | 0.0323 | 0.0272 |
| *R*1; *wR*2[$I > 2\sigma(I)$] | 0.0423; 0.0925 | 0.0513 ; 0.1210 | 0.0410 ; 0.1037 | 0.0365; 0.0833 |
| *R*1; *wR*2 (all data) | 0.0582; 0.1368 | 0.0735 ; 0.1580 | 0.0573 ; 0.1604 | 0.0476; 0.1151 |

**Table 2.** Selected bond distances (Å) and angles (deg) for compounds **1-4**

| $C_{22}H_{18}N_{10}ZnF_{12}P_2$ **(1)** | $C_{34}H_{46}N_{14}O_4CdF_{12}P_2$ **(2)** | $C_{22}H_{22}N_{12}O_8Cd$ **(3)** | $C_{22}H_{26}N_{11}O_7CdF_6P$ **(4)** |
|---|---|---|---|
| Zn(1)-N(1) 2.014(3) | Cd(1)-N(1) 2.283(3) | Cd(1)-N(1) 2.313(4) | Cd(1)-N(5)#1 2.295(3) |
| Zn(1)#2-N(5) 2.017(3) | Cd(1)-N(6) 2.295(3) | Cd(1)-N(5) 2.353(5) | Cd(1)-N(1) 2.365(3) |
| Zn(1)-N(6) 2.024(4) | Cd(1)-N(5)#2 2.332(4) | Cd(1)-O(1) 2.317(4) | Cd(1)-O(1) 2.371(3) |
| Zn(1)-N(9) 2.000(4) | Cd(1)-N(10)#1 2.325(4) | N(1)-Cd(1)-N(1)#1 180 | N(5)#1-Cd(1)-N(5)#2 180 |
| N(9)-Zn(1)-N(1) 98.32(15) | Cd(1)-O(1) 2.374(3) | N(1)-Cd(1)-O(1) 91.66(15) | N(5)#1-Cd(1)-N(1) 93.44(12) |
| N(9)-Zn(1)-N(5)#2 120.12(15) | Cd(1)-O(2) 2.376(3) | N(1)#1-Cd(1)-O(1) 88.34(15) | N(5)#2-Cd(1)-N(1) 86.56(12) |
| N(1)-Zn(1)-N(5)#2 114.63(14) | N(1)-Cd(1)-N(6) 178.59(13) | O(1)-Cd(1)- O(1)#1 180.0 | N(5)#1-Cd(1)-O(1)#3 87.42(12) |
| N(9)-Zn(1)-N(6) 117.42(14) | N(1)-Cd(1)-N(10)#1 89.98(13) | N(1)-Cd(1)-N(5)#1 83.96(16) | N(5)#2-Cd(1)-O(1)#3 92.58(12) |
| N(1)-Zn(1)-N(6) 108.57(14) | N(6)-Cd(1)-N(10)#1 89.14(13) | N(1)#1-Cd(1)-N(5)#2 96.04(16) | N(1)-Cd(1)-O(1)#3 88.58(11) |
| N(5)#2-Zn(1)-N(6) 98.18(15) | N(1)-Cd(1)- N(5)#2 90.93(13) | O(1)-Cd(1)- N(5)#2 91.71(15) | N(1)#3-Cd(1)-O(1)#3 91.42(11) |
| | N(6)-Cd(1)-N(5)#2 89.92(13) | O(1)#1-Cd(1)- N(5)#2 88.29(15) | O(1)#3-Cd(1)-O(1) 180 |
| | N(10)#1-Cd(1)-N(5)#2 177.78(13) | N(5)#2-Cd(1)-N(5)#3 180 | |
| | N(1)-Cd(1)-O(1) 85.08(12) | | |
| | N(6)-Cd(1)-O(1) 96.06(12) | | |
| | N(10)#1-Cd(1)-O(1) 93.00(12) | | |
| | N(5)#2-Cd(1)-O(1) 89.10(12) | | |
| | N(1)-Cd(1)-O(2) 94.77(12) | | |
| | N(6)-Cd(1)-O(2) 84.12(12) | | |
| | N(10)#1-Cd(1)-O(2) 88.83(12) | | |
| | N(5)#2-Cd(1)-O(2) 89.08(12) | | |
| | O(1)1-Cd(1)-O(2) 178.16(11) | | |

Symmetry transformations used to generate equivalent atoms:

**1**. #1 -x,-y,-z+2 #2 -x+1,-y,-z+1

**2.** #1 x+1/2,-y+1/2,z-1/2 #2 x-1/2,-y+1/2,z+1/2

**3.** #1 -x+1,-y,-z+1 #2 x,-y+1/2,z+1/2 #3 -x+1,y-1/2,-z+1/2

**4.** #1 x+1/2,-y+2,z-1/2 #2 -x+3/2,y,-z+1/2 #3 -x+2,-y+2,-z

**Table 3:** Hydrogen bonding interaction parameters in **1, 3** and **4**

| (D-H···A) | *d* (H···A) (Å) | *d* (D···A) (Å) | < (D-H···A)(°) |
|---|---|---|---|
| | | **1** | |
| C3-H3··· F10 | 2.43 | 3.355(6) | 171 |
| C20-H20···F11 | 2.45 | 3.327(7) | 157 |
| | | **3** | |
| C3-H3···O3 | 2.57 | 3.337(7) | 163 |
| O1-H1A···O3 | 1.88(8) | 2.732(5) | 178(10) |
| | | **4** | |
| O1-H101···O2 | 1.93 | 2.754(4) | 168 |
| O2-H202···O3 | 1.83(5) | 2.696(6) | 169(4) |

**1.** F11 is at equivalent position x, -1 + y, z.

**3.** O3 is at equivalent position -1 + x, y, z.

**4**. O3 is at 3/2 - x, y, 3/2 – z.

**References**


(1) J.-R. Li, J. Sculley and H.-C. Zhou, *Chem. Rev.*, 2012, **112**, 869.

(2) S. R. Batten, M. S. Neville and D. R. Turner, *Coordination Polymers: Design, Analysis and Application*; RSC: Cambridge, 2009.

(3) G. Férey, *Chem. Soc. Rev.*, 2008, **37**, 191.

(4) R. Custelcean and B. A. Moyer, *Eur. J. Inorg. Chem.*, 2007, 1321.

(5) D. Bradshaw, J. B. Claridge, E. J. Cussen, T. J. Prior and M. J. Rosseinsky, *Acc. Chem. Res.*, 2005, **38**, 273.

(6) S. Kitagawa, R. Kitaura and S. Noro, *Angew. Chem. Int. Ed.*, 2004, **43**, 2334.

(7) J.-P. Zhang, P.-Q. Liao, H.-L. Zhou, R.-B. Lin and X.-M. Chen, *Chem. Soc. Rev.*, 2014, **43**, 5789.

(8) G. K. Kole and J. J. Vittal, *Chem. Soc. Rev.*, 2013, **42**, 1755.

(9) W.L. Leong and J. J. Vittal, *Chem. Rev.*, 2011, **111**, 688.

(10) J. J. Vittal, *Coord. Chem. Rev.*, 2007, **251**, 1781.

(11) M. Kawano and M. Fujita, *Coord. Chem. Rev.*, 2007, **251**, 2592.

(12) S. Neogi, S. Sen and P. K. Bharadwaj, *CrystEngComm*, 2013, **15**, 9239.

(13) X.-F. Wang, Y. Wang, Y.-B. Zhang, W. Xue, J.-P. Zhang and X.-M. Chen, *Chem. Commun.*, 2012, **48**, 133.

(14) C.-B. Ma, M.-Q. Hu, H. Chen, M. Wang, C.-X. Zhang, C.-N. Chen and Q.-T. Liu, *CrystEngComm*, 2010, **12**, 1467.

(15) S. Kitagawa and R. Matsuda, *Coord. Chem. Rev.*, 2007, **251**, 2490.

(16) D. Tanaka and S. Kitagawa, *Chem. Mater.*, 2008, **20**, 922.

(17) C.-P. Li, J. Chen, W. Guo and M. Du, *J. Solid State Chem.*, 2015, **223**, 95.

(18) L. Hashemi and A. Morsali, *CrystEngComm*, 2013, **15**, 8894.

(19) G.-C. Xu, Y.-J. Ding, T. Okamura, Y.-Q. Huang, Z.-S. Bai, Q. Hua, G.-X. Liu, W.-Y. Sun and N. Ueyama, *Cryst. Growth Des.*, 2009, **9**, 395.

(20) G.-C. Xu, Q. Hua, T. Okamura, Z.-S. Bai, Y.-J. Ding, Y.-Q. Huang, G.-X. Liu, W.-Y. Sun and N. Ueyama, *CrystEngComm*, 2009, **11**, 261.

(21) J. Ma, X. Huang, Y. Song, X. Song and W. Liu, *Inorg. Chem.*, 2009, **48**, 6326.

(22) G.-C. Xu, Y.-J. Ding, T. Okamura, Y.-Q. Huang, G.-X. Liu, W.-Y. Sun and N. Ueyama, *CrystEngComm*, 2008, **10**, 1052.

(23) R. Custelcean and B. A. Moyer, *Eur. J. Inorg. Chem.*, 2007, 1321.

(24) M. Du, X.-J. Zhao, J.-H. Guo and S. R. Batten, *Chem. Commun.*, 2005, 4836.

(25) G. Yang and R. G. Raptis, *Chem. Commun.*, 2004, 2058.

(26) E. Bosch, J. Matheny, A. E. Brown and B. Eichler, *CrystEngComm*, 2011, **13**, 5755.

(27) S. Kitagawa and K. Uemura, *Chem. Soc. Rev.*, 2005, **34**, 109.

(28) G. R. Desiraju, *Acc. Chem. Res.*, 2002, **35**, 565.

(29) B. Venkataramanan, M.-A. Saifudin, J. J. Vittal and V. Suresh, *CrystEngComm*, 2004, **6**, 284.

(30) A.V. Muehldorf, D. V. Engen, J. C. Warner and A. D. Hamilton, *J. Am. Chem. Soc.*, 1988, **110**, 6562.

(31) A. Robertazzi, F. Krull, E.-W. Knapp and P. Gamez, *CrystEngComm*, 2011, **13**, 3293.

(32) S. Noro, R. Kitaura, M. Kondo, S. Kitagawa, T. Ishii, H. Matsuzaka and M. Yamashita, *J. Am. Chem. Soc.*, 2002, **124**, 2568.

(33) C.-Y. Chen, P.-Y. Cheng, H.-H. Wu and H. M. Lee, *Inorg. Chem.*, 2007, **46**, 5691.

(34) N. Singh and G. Anantharaman, *CrystEngComm*, 2014, **16**, 6203.

(35) N. Singh and G. Anantharaman, *CrystEngComm*, 2014, **16**, 7914.

(36) B. Hu, T. Tao, Z.-Y. Bin, Y.-X. Peng, B.-B. Ma and W. Huang, *Cryst. Growth Des.*, 2014, **14**, 300.

(37) S. Tripathi, R. Srirambalaji, N. Singh and G. Anantharaman, *J. Chem. Sci.*, 2014, **126**, 1423.

(38) A. Caballero, E. Díez-Barra, F. A. Jalón, S. Merino and J. Tejeda, *J. Organomet. Chem.*, 2001, **617-618**, 395.

(39) V. A. Blatov, Multipurpose crystallochemical analysis with the program package TOPOS, *IUCr CompComm Newsletter*, 2006, **vol. 7**, p. 4, http://www.topos.ssu.samara.ru.

(40) G. M. Sheldrick, *SHELXL-97*, *Program for Crystal Structure Solution and Refinement*; University of Göttingen, Göttingen, Germany, 1997.

(41) G. M. Sheldrick, *SHELXTL Reference Manual*: Version 5.1, Bruker AXS, Madison, WI, 1998.

(42) J.-Y. Lee, C.-Y. Chen, H. M. Lee, E. Passaglia, F. Vizza and W. Oberhauser, *Cryst. Growth Des.*, 2011, **11**, 1230.

(43) C.-L. Chen, A. M. Goforth, M. D. Smith, C.-Y. Su and H. C. Zur Loye, *Inorg. Chem*., 2005, **44**, 8762.

(44) N. Masciocchi, C. Pettinari, E. Alberti, R. Pettinari, C. D. Nicola, A. F. Albisetti and A.Sironi, *Inorg. Chem*., 2007, **46**, 10501.

(45) D. Michael, P. Mingos and A. L. Rohl, *J. Am. Chem. Soc.*, 1983, **105**, 5220.

(46) M. D. Allendorf, C. A. Bauer, R. K. Bhakta and R. J. T. Houk, *Chem. Soc. Rev.*, 2009, **38**, 1330.

(47) Y. Cui, Y. Yue, G. Qian and B. Chen, *Chem. Rev.*, 2012, **112**, 1126.

(48) J. Heine and K. Müller-Buschbaum, *Chem. Soc. Rev.*, 2013, **42**, 9232.

(49) B. Chen, Y. Yang, F. Zapata, G. Qian, Y. Luo, J. Zhang and E. B. Lobkovsky, *Inorg. Chem.*, 2006, **45**, 8882.

## Table of Contents Use Only

# Anion Triggered and Solvent Assisted Structural Diversity and Reversible Single Crystal to Single Crystal (SCSC) transformation between 1D and 2D Coordination Polymers

*Sarita Tripathi, Renganathan Srirambalaji, Samir Patra and Ganapathi Anantharaman*[a]*

[a] Department of Chemistry, Indian Institute of Technology, Kanpur-208016, INDIA

---

Synthesis of four new coordination polymers (CPs) $\{[Zn(pyim_2)_2]\cdot(PF_6)_2\}_n$ (**1**) (1D), $\{[$*trans*-$Cd(pyim_2)_2(DMF)_2]\cdot(PF_6)_2\cdot(DMF)_2\}_n$ (**2**) (1D), $\{[$*trans*-$Cd(pyim_2)_2(H_2O)_2]\cdot(NO_3)_2\}_n$ (**3**) (2D) and $\{[$*trans*-$Cd(pyim_2)_2(H_2O)_2]\cdot(PF_6)\cdot(NO_3)\cdot(H_2O)_2\}_n$ **(4)** (1D) starting from angular ditopic ligand 2,6-bis(imidazol-1-yl)pyridine ($pyim_2$) and the anion triggered structural variation (1D and 2D) under different solvent conditions have been reported.